ELSEVIER

Journal of Nuclear Materials 276 (2000) 104–113

journal of nuclear materials

www.elsevier.nl/locate/jnucmat

Stability of ordered phases under irradiation

C. Abromeit[a,*], H. Wollenberger[a], S. Matsumura[b], C. Kinoshita[b]

[a] *Hahn-Meitner-Institut Berlin GmbH, Glienicker Str. 100, D-14109 Berlin, Germany*

[b] *Department of Applied Quantum Physics and Nuclear Engineering and Department of Energy Science and Engineering, Kyushu University 36, Fukuoka 812-8581, Japan*

Abstract

The present paper reviews recent results of experiments and modelling on phase changes of $L1_2$ ordered alloys under energetic particle irradiation. The temperature dependence of the various processes are discussed for the single phase Ni_3Al as well as for the precipitated phase in a disordered solid solution. Treated are the size of the cascade-induced disordered zones, the ordering efficiency by point defect migration, the disordering kinetics for overlapping cascade damage and the disordering and dissolution of γ' precipitates in a Ni base alloy.

1. Introduction

Precipitates of ordered intermetallic phases are used as strengthening particles in technical alloys. Radiation-induced destruction of ordered precipitates causes a significant degrading of the mechanical properties. Therefore, quantitative understanding of the underlying processes is required for life-time predictions valid for given radiation environments.

The theoretical understanding of the stability of precipitated phases has two aspects. One regards the order–disorder reaction in a chemical homogeneous (one phase) alloy. In this case, the driving force for phase changes is the gradient of the degree of order and in addition athermal ballistic atom jumps. Details of cascade evolution and the changes of the degree of order by migrating point defects have been calculated and measured by proper techniques as discussed below. This knowledge is necessary for the successful theoretical treatment of the second aspect, the radiation-induced dissolution of ordered precipitates in a disordered solid solution. Spatial variations of the composition as occurring around the interface between precipitate and solution induce additional driving forces for the disordering process. As shown below, this interrelation between the degree of order and the composition is crucial for the actual stability of the ordered precipitated phase and therefore for their applicability in structural reactor materials.

For some intermetallic phases, the experimental results can be compared with MD simulations of the radiation-induced atomic rearrangement [1–11]. An example of a 10 keV displacement cascade in a long-range ordered Ni_3Al alloy at $T = 20$ K is given in Fig. 1(a), which shows all displaced atoms, such as displaced to correct lattice sites (white circles) and such as ended up at 'wrong' lattice sites (dark circles) [11]. The disordered volume built by wrongly placed atoms causes a dark speckle in a TEM dark-field image. Its size may be measured and compared with results of MD simulation [12–14].

In Fig. 1(b) the distribution of vacancies and interstitials produced by the cascade of Fig. 1(a) is shown. Such defect structures are well known from cascade damage in pure metals or in disordered alloys. The majority of replacement collisions do not leave obvious traces there. In ordered materials, however, the spatial distribution of the degree of order presents a detailed trace of the collision cascade evolution.

In the present paper, we discuss the temperature dependence of the stability of ordered Ni_3Al under cascade-producing irradiation. Measured sizes of single well-separated disordered zones are discussed in terms of

* Corresponding author. Tel.: +49-30 8062 2825, fax: +49-30 8062 3059.

E-mail address: abromeit@hmi.de (C. Abromeit)

0022-3115/00/$ - see front matter
PII: S0022-3115(99)00173-7

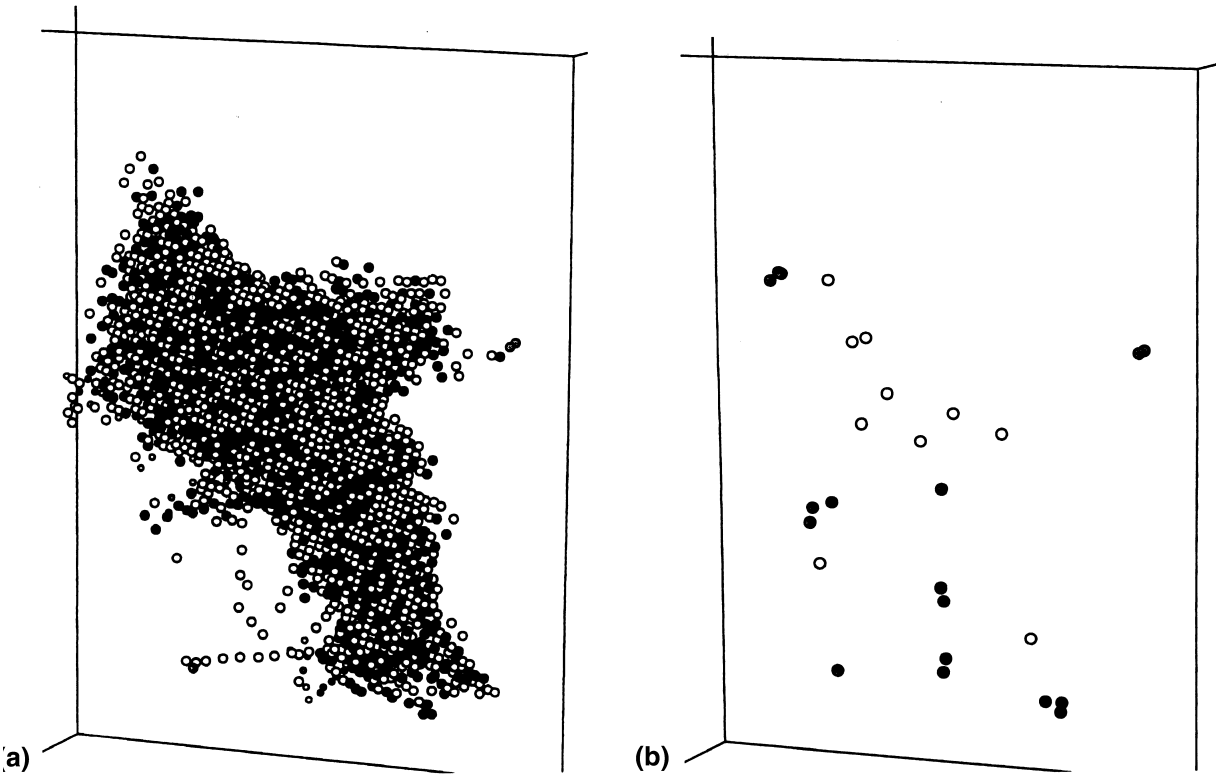

Fig. 1. (a) Three-dimensional reconstruction of a 10 keV cascade in Ni_3Al simulated by means of molecular dynamics simulation.The circles give replaced atoms, dark – antisite atoms, white – atoms on correct sublattice positions (for details see Ref. [11]). (b) Vacancies and interstitials produced by the cascade shown in Fig. 1(a).

a thermal spike model approach, the effect of overlapping of disordered zones and the radiation-induced reordering by point defect migration are estimated. It is further shown how the stability of ordered precipitates in a solution of different composition is degraded under irradiation by the composition gradient.

2. Evolution of atomic disorder within single cascades

The disordered zones observed in an ordered crystal result from collision cascades followed by subsequent thermalisation and energy dissipation. In the collisional phase of the cascade, the atomic jump processes are dominated by athermal, ballistic jumps, which produce a large amount of chemical and structural disorder. The size of the volume damaged in this short collisional phase increases with increasing particle energy, but is nearly independent of the sample temperature [3,15].

These zones evolve according to the recoil energy dissipation. For the calculation of the final size of the disordered zones, modelling of the evolution according to a thermal spike [16] is a helpful approach. The energy dissipation is assumed to cause a temperature profile $T(r,t)$. The degree of local order $S(r,t)$ is then determined by the enhanced local atomic mobility $M(T(r,t))$ and by the local thermodynamic function $F(T(r,t))$.

2.1. The thermal spike model

This model is a well known means to describe the time-spatial energy evolution $E(r,t)$ in a cascade after completion of the collisional phase. It assumes that the energy in larger cascades is rapidly thermalized so that the temperature $T(r,t)$ can be defined according to the equipartition rule $E(r,t) = 3k_BT/2$. The temperature profile is obtained according to the heat conduction equation with the initial condition given by the energy distribution at the end of the collisional phase. This approach fits well with MD calculations in various metallic systems i.e. Cu, Ni, Ni_3Al [2–11]. The parameter of reference is the thermal conductivity k/c, which may be determined by comparison with MD simulation. A typical result is $k/c \approx 3 \times 10^{-7}$ m^2/s, which is two orders of magnitude smaller than that for bulk Ni at room temperature (RT) [3].

Several attempts of calculation have been made for the time evolution of local order according to the localized heating and cooling. Two contributions of atomic motion have to be considered: (i) jumps in a homogeneous state of order, and (ii) jumps driven by the gradient of the state of order. A theoretical approach has been developed by Matsumura and co-workers [17–19], using time-dependent Ginzburg Landau equations to calculate both the local order parameter and the local composition. A similar approach based upon kinetic master equations of the Bragg Williams type has been reported by Bakai and co-workers [20]. These models allow to calculate details of order profiles $S(r,t)$, which are not accessible experimentally yet.

In order to estimate the influence of the irradiation temperature on the disordered zone size we assume that in Ni_3Al disordering ($S=0$) occurs when the spike temperature in the heating phase exceeds the critical temperature T_c, and that reordering to $S=1$ occurs as soon as the temperature falls below T_c during the cooling phase. As for Ni_3Al $S=1$ holds up to the melting temperature we may take $T_c = T_{melt}$, i.e. reordering occurs simultaneously to solidification.

With this assumption we have calculated the time evolution of the (spherical) volume for which $T > T_{melt}$ [21,22]. The result is shown in Fig. 2. The maximum radius of the molten zone increases with increasing sample temperature, i.e. the maximum disordered zone size increases correspondingly. During the subsequent cooling phase with $T < T_c$ atomic replacements will enhance the degree of order (reordering). If the number of jumps necessary for reordering were independent of temperature, the size of the quenched zones of disorder would decrease with increasing irradiation temperature. This behaviour is shown by full symbols in Fig. 2, which indicate schematically the expected sizes of the frozen-in disordered zone for different irradiation temperatures. They correspond to the region where just one ordering jump per site has occurred (see [21]).

2.2. Experimental information

Disordered zones due to displacement cascades have been investigated experimentally in detail by TEM for $L1_2$ ordered intermetallic compounds such as Cu_3Au, Ni_3Al and $Ni_3Al_{1-x}Fe_x$ [12–14,22–26]. Stereo transmission electron microscopy has been used to characterize for thin foil specimens the depth distribution of size and shape of the disordered zones and associated dislocation loops [23–26]. For the zone size, independence of depth was found in Ni_3Al irradiated by 50 keV Ta^+ ions at 573 K (Fig. 3). Zones situated close to the sample surface appear to be more elongated along the incident beam direction than those in greater depth and are not taken into account for the zone size determination. The mean size distribution in the interior has been determined for different irradiation temperatures, 30 K $< T <$ 880 K, different ion species (Kr, Xe, Ni, Ta ions) and ion energies between 30 and 300 keV [22]. The temperature dependence of the disordered zone size has been reported for 50 keV ion irradiated Ni_3Al [22–26]. The zones were observed by dark-field imaging with the $\langle 1\,0\,0\rangle$ superlattice reflection. The average diameters of zones are shown in Fig. 4. Between 30 K and RT the size increases and above RT it decreases with increasing temperature. This behaviour agrees qualitatively with the predictions of the thermal spike model (see Fig. 2).

2.3. Limitations of the theoretical descriptions

A number of simplifying assumptions made for the modelling impede the correct quantitative analysis of the size. The problems not yet treated successfully are:

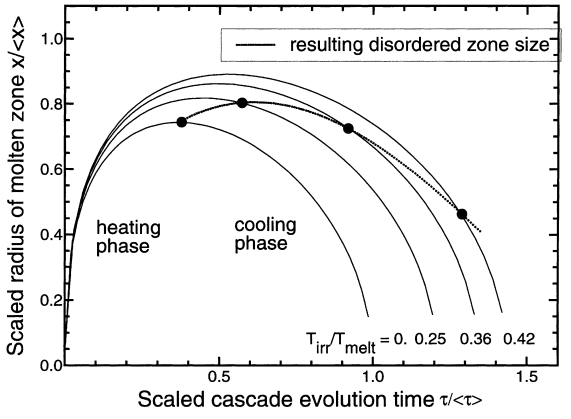

Fig. 2. Time evolution of the molten zone radius. Full circles give estimated frozen-in disordered zones. The dotted line shows the temperature dependence schematically (see Ref. [22]).

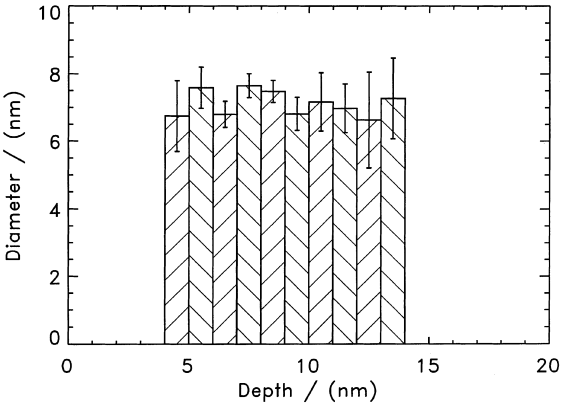

Fig. 3. Mean diameter d of disordered zones as a function of depth in a Ni_3Al foil sample (50 keV Ta^+ ions, irradiation temperature 573 K) [24].

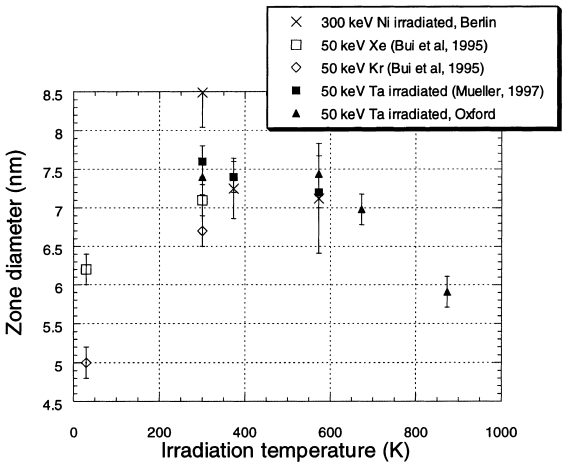

Fig. 4. Average diameter of disordered zones in Ni_3Al according to Ref. [22].

disordering by dislocation loop production, reordering at low temperatures due to high local point defect concentrations, and reordering jumps not occurring just at the interface between molten zone and solid. Due to local point defect annihilation inside the cascade at temperatures below the melting temperature, some ordering jumps will produce a certain state of order also inside the disordered volume. The assumed sharp transition between the ordered matrix and the disordered cascade core is a first order approximation only. However, the experimentally observed disordered zones do not indicate that there is significant reordering inside the cascade [22–26]. MD simulation confirms this assumption [3–11].

Another serious problem exists with the assumption of local thermodynamic parameters such as the critical temperature T_c for a limited volume and for the life time of the thermal spike. We have experimentally varied T_c by partially substituting Al by Fe. In contrast to the theoretical prediction the disordered zone size was not observed to be altered significantly for 50 keV Ta ions [26]. This discrepancy may arise from one of the above quoted simplifying assumptions.

Results of computer simulations by Gao and Bacon [27] seem to disagree with these experimental findings. While the obtained temperature dependence of the molten zones agrees with that predicted by the thermal spike model, that of the disordered zones (90% of the antisite atoms) does not. In the MD simulations, its size exceeds that of the molten zone in contrast to the thermal spike model and does not decrease with increasing temperature as found experimentally. The volume formed by the antisite atoms may not be the same as that seen by TEM analysis. Calculated TEM images of the MD results would be helpful for a comparison of experimentally determined disordered zone sizes.

3. Disordering by overlapping cascades

3.1. Modified thermal spike model for high fluence

At higher fluences the reordering process occurring during the cooling phase may take place more and more in disordered environments left by earlier cascade events. This effect must certainly be considered. In the above quoted thermal spike approach [21] reordering is assumed to occur in the same manner irrespective of whether the cascade is produced in an ordered region or in an already disordered region. Then, the average degree of order reaches a stationary value after prolonged irradiation $S(T) = 1 - V_d/V_{max}$ which depends only on the ratio of the disordered volume V_d to the maximum disordered volume V_{max}.

In the modified thermal spike model [25,28], the disordering kinetics are approximated by

$$\frac{\partial S}{\partial t} = -\varepsilon K S + \kappa(t,T)\left[\varepsilon K S_\infty(T) + \left.\frac{\partial S}{\partial t}\right|_{\text{re-ordering}}\right], \qquad (1)$$

where $\kappa = \kappa(t,T)$ is the modification factor for the reduced reordering at higher fluences. The third term on the right-hand side of Eq. (1) describes the radiation-enhanced thermal reordering by migrating point defects. It is important for higher temperatures when vacancies are mobile and contribute to the ordering process. The vacancy contribution is taken into account by using an approach given by Banerjee and Urban [29]. Whether migrating interstitials contribute to reordering is discussed in the following.

In most alloys the interstitial mobility is much larger than that of vacancies. Since the experimental results of the disordering in electron-irradiated Ni_3Al give hints on reordering at lower temperatures [30,31] at which vacancies are not mobile, it has to be checked whether reordering might be caused by interstitial migration. As for the vacancy mechanism we assume

$$\left.\frac{\partial S}{\partial t}\right|_{\text{re-ordering}} = \alpha_i c_i \nu_i f(S) + \alpha_v c_v \nu_v f(S), \qquad (2)$$

where $c_{i,v}(t)$ is the time-dependent concentration, $\nu_{i,v}$ the jump frequency, and $\alpha_{i,v}$ is the ordering efficiency factor of interstitials and vacancies, respectively. For the purpose of this investigation, the free energy functional $f(S)$ has been assumed to be independent of the type of the ordering jump process and is therefore taken to be the same as under thermal conditions.

The kinetics of production and annihilation of the interstitials in Ni_3Al after electron irradiation have been investigated by Dimitrov and co-workers using electrical resistivity measurements [32,33]. In agreement with MD calculations [1–3] they conclude the existence of several types of interstitials with different symmetries and activation energies for migration. The most stable

configuration is the Ni–Ni dumbbell. This configuration migrates three dimensionally on the Ni-sublattice with a low activation energy (0.10–0.15 eV). For the completely ordered structure there may be another Ni*–Ni dumbbell of a different symmetry, which migrates two dimensionally forming temporarily mixed dumbbells Al*–Ni. The migration energy of this kind of dumbbell was estimated to be 0.31 eV. No other long-range migrating interstitial type defect is observed in a completely ordered alloy. As the re-ordering rate has to be calculated for an alloy in the non-equilibrium state of partial order, i.e. for $S<1$, the use of defect properties in the stoichiometric ordered alloys can only be considered as a first approximation.

Defect reactions in a system under irradiation are the production, the recombination of vacancies and interstitials, and the annihilation of the migrating point defects at permanent sinks. They may be described by a chemical reaction scheme [34,35] resulting in a coupled set of rate equations for the time evolution of the average concentrations of vacancies and interstitials.

The effect of reordering under irradiation becomes experimentally detectable only for sufficiently high fluences Φ, e.g. for electron irradiation at $\Phi > 0.3$ dpa and for ion irradiation at $\Phi > 0.02$ dpa [36]. By using equal sink strengths for vacancies and interstitials, the evolution of the interstitial concentration up to these fluences is approximately given by

$$c_i(\Phi)v_i = \frac{a}{\sqrt{\Phi}} \gg c_v(\Phi)v_v \quad \text{with } a = \frac{1}{16\pi}\sqrt{\frac{\eta}{2c_s}}, \tag{3}$$

where c_s is the sink concentration for interstitials and η is the fraction of freely migrating interstitials. They depend on the type of the irradiation [37]. For electrons, only single point defects are produced ($\eta = 1$) whereas ion or neutron irradiation produces cascades and the fraction of freely migrating interstitials is much smaller ($0.01 < \eta < 0.05$) due to spontaneous recombination and clustering in the cascades.

For electron irradiation, no drastic temperature dependence of the sink density is expected below 300 K. Consequently, the observed temperature dependence of the ordering rate has to be attributed to a temperature-dependent reordering efficiency α_i [38].

For an approximate estimation of α_i, a simple kinetics equation for the reordering was assumed [39]

$$\frac{d}{d\Phi}S = -\varepsilon S + \frac{c(1-S)^2}{\sqrt{\Phi}} \quad \text{with } c = \alpha_i a \tag{4}$$

with the initial condition $S(0) = 1$. In order to obtain the parameter c for the temperature range between 200 and 300 K, Eq. (4) is fitted to the electron irradiation results of Liu and Mitchell [30,31] and of Butler and Orchard [40]. The fitted values $c(T)$ are shown in an Arrhenius plot in Fig. 5. A straight line fit to these values yields an activation energy of 0.075 eV. Extrapolation to 300 K results in $c = 1.62$, which is in agreement with the experimental data of Butler and Orchard [40].

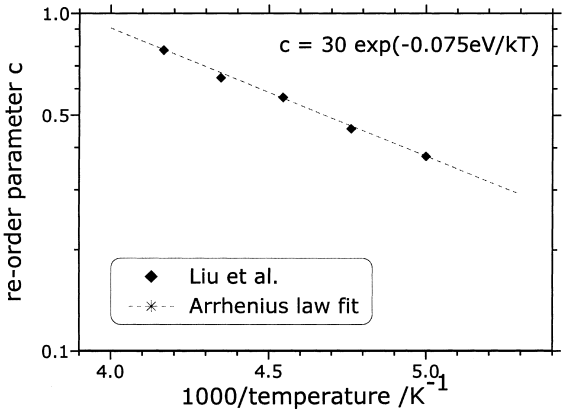

Fig. 5. Arrhenius plot of the reordering efficiency c (Ref. [38]).

No information exists on the effective ordering step based on interstitial migration. However, the following configuration would fulfil the conditions derived above. A Ni–Ni dumbbell interacts with two neighbouring antisites Ni_{Al} and Al_{Ni} during its migration. It replaces the involved atoms to their correct sites and retains its Ni–Ni dumbbell configuration. The activation energy 0.075 eV quoted above is then the energy barrier which has to be overcome for the atomic replacement from the antisites to the correct ones. MD investigations might help to clarify the effective ordering mechanism.

For ion irradiation ($\epsilon = 30$) [36] the reordering effect by long-range migrating interstitials is too small to produce a measurable state of LRO. In order to obtain a significant state of order, e.g. $S = 0.135$ at 1 dpa at RT, the parameter c should be larger than 5. In contrast, using $\eta = 0.05$ and sink density $c_s = 10^{-5}$ at 300 K valid for the ion irradiation, $c = 0.05$ i.e. a completely disordered state is expected at RT at a fluence of 1 dpa. However, a non-vanishing degree of order has been detected even after higher fluences under 300 keV Ni^+ irradiation. The thermal spike model can explain the experimentally observed results [25,28,41].

3.2. The average LRO order of the irradiated single phase alloy

Disordering by cascades can be simulated by a Monte Carlo calculation [42]. Disordered zones are modelled by a statistical redistribution of atoms inside a cascade volume. The cascades are created randomly in an initially completely ordered volume of $L1_2$ structure. Periodic boundary conditions are used. For the period elapsing between two consecutive cascades, thermally activated ordering of disordered regions by means of

statistically distributed atomic replacements is assumed according to the interaction parameters of the $L1_2$ structure, $V_1 = -122.30$, $V_2 = -6.0$, $V_3 = 16.58$, and $V_4 = 6.82$ [43]. Fig. 6 shows, for example, 50 replacement cascades after 10 Monte-Carlo steps. For such a configuration the intensities of superlattice reflections may be derived from a two-dimensional Fourier transform of the MC result. They decay with the number of generated cascades and are a direct measure of the average state of order and can be compared with experimentally determined superlattice reflections (SLR).

Disordering and subsequent reordering of the $L1_2$ structure of Ni_3Al has been investigated by means of TEM [25,28,41]. From the intensities of superlattice reflections in selected area diffraction, the average degree of the order was determined. The dynamical diffraction theory was applied by means of the EMS-Software [44]. Local variations of the ordered state are not resolved by this method.

The intensities of the reflections by TEM were measured by means of imaging plates (Fuji), which were read out by the Fuji scanners 'BAS 1000' and 'FDL 5000'. The intensity profiles were fitted by Lorentz functions to evaluate integrated intensities of the fundamental and superlattice reflections (FR and SLR, respectively).

3.3. Experimental disordering of the irradiated single phase alloy

TEM specimens of Ni_3Al were irradiated with 300 keV Ni^+ ions up to fluences of 10 dpa at temperatures between 100 and 773 K [25,28,41]. The displacement rate was 2.5×10^{-3} dpa s^{-1}. The disordering of initially ordered Ni_3Al is shown in Fig. 7. The temperature dependence of the kinetics indicates the maximum disordering efficiency at RT. Below RT, complete disorder is obtained after fluences larger than 1 dpa. Above RT, a given degree of disorder can be attained only for fluences increasing with increasing irradiation temperature.

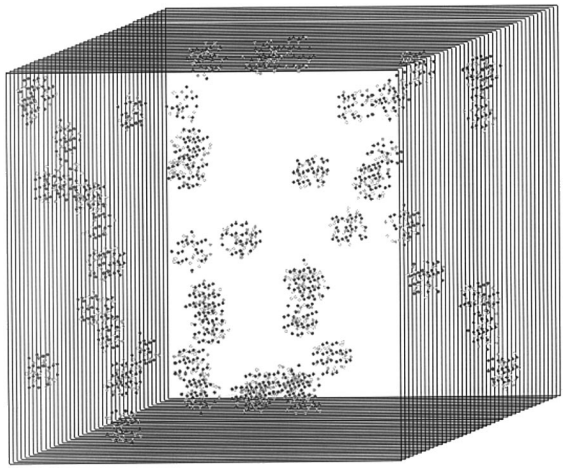

Fig. 6. MC simulation of disordered zones in Ni_3Al. For details see text.

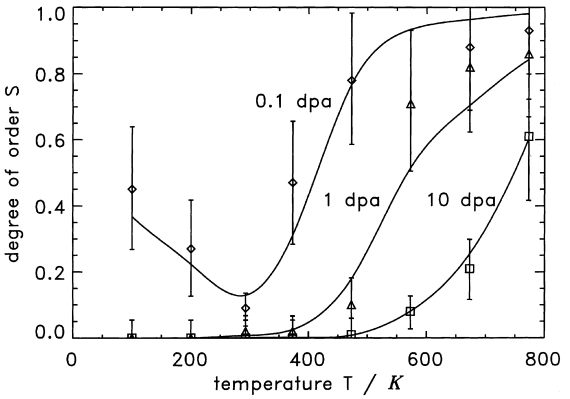

Fig. 7. Temperature dependence of the LRO parameter of Ni_3Al disordered by 300 keV Ni^+ irradiation after fluences 0.1, 1 and 10 dpa. The curves are fits according to the modified thermal spike model with an efficiency function $\kappa(t, T)$ as shown in Fig. 8.

The results (see Fig. 7) for low fluences $\Phi = 0.1$ dpa fit to the size dependence of disordered zones measured by TEM directly as discussed in the last section (see Fig. 3). At temperatures below RT the volume of the disordered zone produced by single cascades increases with temperature rise. As the disordering efficiency κ for low temperature irradiation is proportional to the disordered volume V_d, the disordering efficiency increases with increasing temperature. This behaviour is obviously valid up to RT. Above RT the number density and the sizes of disordered zones decrease with increasing temperature, which leads to an increasingly smaller disordering rate.

The experimental results shown in Fig. 7 are in general accordance with earlier qualitative observations under similar irradiation conditions [41]. However, due to the improved data evaluation, the present data allow a quantitative discussion based on the modified thermal spike model [25,28]. The corresponding efficiency $\kappa(t, T)$ is given in Fig. 8. It shows that reordering becomes less efficient for high fluences, i.e. for smaller average degrees of order.

4. Disordering and dissolution of precipitated ordered phases

The mechanical properties of the superalloys depend on the stability of ordered precipitates. Their behaviour in radiation environments has been investigated

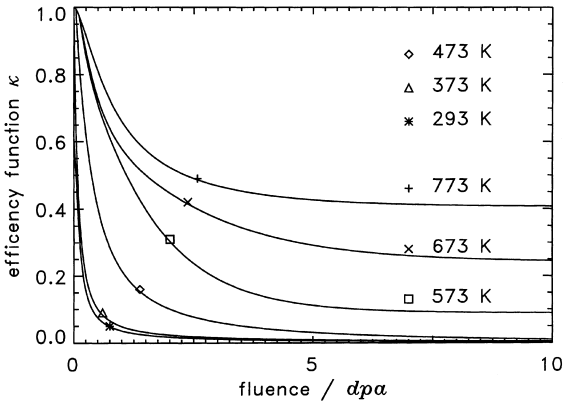

Fig. 8. Fitted efficiency function for reordering $\kappa(t,T)$ versus irradiation fluence according to the modified thermal spike model (fit see Fig. 7).

theoretically and experimentally in great detail (see Ref. [45] for an extensive review of relevant publications until 1984). Recently, theoretical treatments of the coupled change of the composition and of the local degree of order have been reported [46–51] and applied to the evolution of the degree of order inside the precipitate and the composition profile around the precipitate as a function of irradiation parameters. Experimentally, the degree of order and of the composition of irradiated γ' precipitates in Nimonic PE16 were determined by two techniques [53–56]. Field ion microscopy with atom probe (FIM-AP) was used to resolve the compositional dissolution [54,55,57], and TEM was used to determine the average degree of order [52,55].

4.1. Combined application of FIM-AP and TEM

By FIM-AP the specimen tip is field evaporated atomic layer by atomic layer and the evaporated atoms (ions) are analysed with respect to their chemical identity by means of a time of flight mass spectrometer. The profiles of γ' precipitates (radius 3.5 nm) have been measured with atomic resolution as a function of fluence and temperature. The observed data have been explained quantitatively by assuming a ballistic interdiffusion process as expected for radiation-induced atomic mixing [56].

Under the same irradiation conditions, TEM measurements were performed on material with the same precipitated volume fraction, but with larger precipitates (radius 10 nm) [52]. Very strong intensities of the superlattice reflections were observed at 573 K and 10 dpa indicating that a large volume fraction of ordered material must be present.

From these observations it has been concluded that the interdiffusion profiles at temperatures above $T > 540$ K should deviate from the Gaussian shape expected from the ballistic mixing only. There must be deviations due to the thermally activated interdiffusion which stabilizes central volume fractions of a precipitate within the composition range of the long-range ordered γ' phase [56,57].

4.2. Theory of simultaneous disordering and dissolution

Matsumura and co-workers describe the simultaneous dissolution and disordering by simple equations based on a time-dependent Ginzburg–Landau (TDGL) model [17–19,49–51]. This approach explains the precipitate evolution under irradiation with two well-known phenomenological radiation parameters, the interdiffusion coefficient due to atomic mixing D_{mix} [37,58] and the disordering efficiency ε [36]. The composition X and the degree of long-range order S are taken to be continuous variables of space and time. The time evolution reads for both quantities

$$\frac{\partial X}{\partial t} = D^{\mathrm{mix}}\nabla^2 X + L(T,\phi)\nabla^2\left(\frac{\delta F(\{X,S,T\})}{\delta X} - \mu\right), \quad (5)$$

$$\frac{\partial S}{\partial t} = -\varepsilon\phi S - M(T,\phi)\frac{\delta F(\{X,S,T\})}{\delta S}, \quad (6)$$

where ϕ is the atomic displacement rate, $F(\{X,S,T\})$ the thermodynamic potential, and μ is the chemical potential. The first terms on the right-hand side of Eqs. (5) and (6) represent atomic diffusion and disordering due to the ballistic jumps induced by irradiation, and the second one the thermodynamical driving force approaching the equilibrium state through the thermally activated process of atomic replacement. The thermal diffusion mobility L and the ordering rate M include the radiation-enhanced thermally activated atom transport at elevated temperatures.

The thermodynamic potential is taken as

$$F[\{X(\mathbf{r}),S(\mathbf{r}),T\}] = \int\left\{f(X,S,T) + \frac{H(T)}{2}(\nabla X)^2 + \frac{K(T)}{2}(\nabla S)^2\right\}\mathrm{d}\mathbf{r} \quad (7)$$

with $f(X,S,T)$ being the mean field free energy density, and H and K are positive constants of the interfacial energy coefficients for varying X and S. If the order–disorder transition is of the second kind and the disordered phase has no tendency to decomposition, the simplest form of $f(X,S,T)$ is given by the Landau expansion,

$$f(X,S,T) = f_0 + \frac{a(T)}{2}\Big\{(X - x_{\mathrm{m}})^2 - b(T) \times\Big\{x_0(T)^2 - X^2\Big\}S^2 + b(T)^2 x_1(T)^2 S^4\Big\}, \quad (8)$$

where f_0 is the mean field free energy of the disordered phase with composition x_m, and a, b and x_1 are positive factors depending on temperature T. Here, $X = 0$ gives the stoichiometric composition for the ordered structure. Details can be found in Refs. [17–19,49–51] where several examples of the stability of a tri-critical system with and without irradiation are treated.

The steady-state solution defines the dynamical phase diagram which is shown in Fig. 9. It is essentially the same phase diagram as discussed by Martin and coworkers [59–61] for an ordered alloy under external forcing, i.e. irradiation.

4.3. Calculated dissolution profiles and disorder kinetics

The evolution of composition and degree of order in and around an ordered precipitate in a disordered matrix was studied by solving numerically the kinetic equations for a one-dimensional array of 250 elements and periodic boundary conditions (see Fig. 10). An approximate solution for spherical precipitates is published in [57].

The curves show a strong decrease of the degree of order for $\Phi = 0.1$ dpa while the shape of the precipitate has not changed much. For $\Phi > 0.1$ dpa, the precipitate is dissolved continuously by the atomic mixing effect. This successive disordering and dissolution was indeed observed for the γ' in the temperature range up to 540 K. The precipitates first vanished in the dark field image before the contrast also started to vanish in the bright field image.

For higher temperatures, however, when the precipitates dissolve in an ordered state, the composition profile shows a sharp interface between ordered and disordered phases. The precipitate shrinks, keeping a significant volume fraction of material in the ordered state. For a discussion of the FIM-AP experimental data

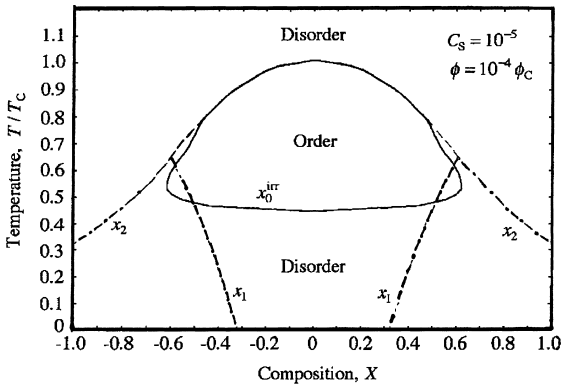

Fig. 9. Dynamical phase diagram for the binary alloy under irradiation with the irradiation parameters indicated. x_1 and x_2 are the thermal equilibrium phase boundaries.

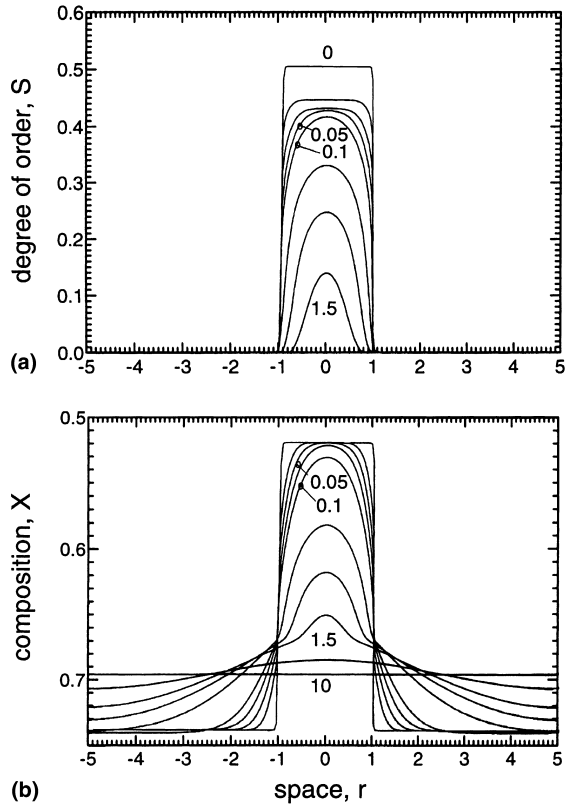

Fig. 10. Precipitate dissolution profiles for elevated temperature. Evolution of S and X for a simulated long-range ordered precipitate (one-dimensional geometry) at $T = 0.5T_c$, (the curves are calculated for $\Phi = 0.01, 0.025, 0.05, 0.1, 0.5, 1.0, 1.5, 2.5, 10$ dpa. Corresponding three-dimensional profiles are published in [57].

of γ' precipitate dissolution in Nimonic PE16 at $T > 540$ K non-Gaussian composition profiles have to be used in order to calculate the corresponding correlation coefficients [57].

5. Summary

Radiation-induced disordering with cascades has been studied during recent years predominantly for Ni_3Al. In the LRO structure collision cascades produce disordered zones the sizes of which depend on the irradiation temperature. This temperature dependence is successfully explained by a thermal spike model which introduces a significant reordering during the thermal spike's cooling phase. The irradiation temperature enters as a boundary condition for the time evolution of the spatial temperature distribution and, hence, the volume elements in which atomic ordering occurs.

For high fluences cascade-induced disordering and subsequent cooling phase reordering take place in increasingly disordered matter. This continuous change of the boundary condition for the individual cascade will influence the reordering efficiency. A quantitative treatment must also take into account the conventional thermally activated ordering ongoing at the irradiation temperature. By this way the experimental data are satisfactorily explained.

The radiation-induced dissolution of ordered precipitates can be well described by coupled kinetic equations for the local composition $X(r,t)$ and local degree of order $S(r,t)$ in the TDGL form. The predictions of this mesoscopic model are consistent with those of the microscopic theory proposed by Martin and coworkers [46–48].The derived phenomenological parameters successfully explain the findings by means of FIM-AP and TEM.

Acknowledgements

The results presented in this review have benefited from collaboration and scientific exchange programs with the various research groups: HMI Berlin (Germany) with KIPT Kharkov (Ukraine) – WTZ project, Kyushu University (Japan) – Humboldt foundation and the Monbusho program, CEN Saclay (France) – PROCOPE programme, and University Oxford (England) – ARC programme. Substantial contributions by A.S. Bakai, F. Bourdeau, E. Camus, N.V. Doan, M.L. Jenkins, S. Müller, G. Martin, V. Naundorf, N. Wanderka and K. Yasuda have been included and are gratefully acknowledged. The authors thank Dr Gao and Professor Bacon for providing details of their results prior to publication.

References

[1] A. Caro, M. Victoria, R.S. Averback, J. Mater. Res. 5 (1990) 1409.
[2] F. Gao, D.J. Bacon, Philos. Mag. A 67 (1993) 289.
[3] F. Gao, D.J. Bacon, Philos. Mag. A 71 (1995) 43, 65.
[4] H. Zhu, R.S. Averback, M. Nastasi, Philos. Mag. A 71 (1995) 735.
[5] T. Diaz de la Rubia, A. Caro, M. Spaczer, Phys. Rev. B 47 (1993) 11483.
[6] M. Spaczer, A. Caro, M. Victoria, T. Diaz de la Rubia, Phys. Rev. B 50 (1994) 13204.
[7] M. Spaczer, A. Caro, M. Victoria, Phys. Rev. B 52 (1995) 7171.
[8] N.V. Doan, H. Tietze, Nucl. Instrum. and Meth. 102 (1995) 59.
[9] M. Spaczer, A. Almazouzi, R. Schäublin, M. Victoria, Rad. Eff. Def. Solids 141 (1997) 349.
[10] A. Almazouzi, M. Alurralde, M. Spaczer, M. Victoria, Mater. Res. Soc. Symp. 481 (1998) 371.
[11] N.V. Doan, R. Vascon, Rad. Eff. Defects Solids 141 (1997) 363.
[12] M.L. Jenkins, K.-H. Katerbau, M. Wilkens, Philos. Mag. 34 (1976) 1141.
[13] M.L. Jenkins, C.A. English, J. Nucl. Mater. 108&109 (1982) 46.
[14] C.A. English, M.L. Jenkins, Mater. Sci. Forum 15–18 (1987) 1003.
[15] M. Alurralde, A. Caro, M. Victoria, J. Nucl. Mater. 183 (1991) 33.
[16] G.H. Vineyard, Radiat. Eff. 29 (1976) 245.
[17] T. Eguchi, K. Oki, S. Matsumura, in: T. Tsakalakos (Ed)., Phase Transformations in Solids, MRS Symp., vol. 21, Elsevier, Amsterdam, 1983, p. 269.
[18] K. Oki, S. Matsumura, T. Eguchi, Phase Trans. 10 (1987) 257.
[19] S. Matsumura, S. Müller, C. Abromeit, Phys. Rev. B 54 (1996) 6184.
[20] A.S. Bakai, M.P. Fateev, Phys. Stat. Sol. B 158 (1990) 81.
[21] C. Abromeit, H. Wollenberger, J. Nucl. Mater. 191–194 (1992) 1092.
[22] M.L. Jenkins, P. Mavami, S. Müller, C. Abromeit, MRS Fall Meeting, Boston, 1998.
[23] T.X. Bui, I.M. Robertson, M.A. Kirk, Mater. Res. Soc. Symp. Proc. 373 (1995) 63.
[24] S. Müller, M.L. Jenkins, C. Abromeit, H. Wollenberger, Mater. Res. Soc. Symp. Proc. 439 (1997) 325.
[25] S. Müller, thesis, TU Berlin, Germany, 1997.
[26] S. Müller, M.L. Jenkins, C. Abromeit, H. Wollenberger, Philos. Mag. A 75 (1997) 1625.
[27] F. Gao, D.J. Bacon, MRS Fall Meeting, Boston, 1998.
[28] S. Müller, C. Abromeit, S. Matsumura, N. Wanderka, H. Wollenberger, J. Nucl. Mater. 271&272 (1999) 241.
[29] S. Banerjee, K. Urban, Phys. Stat. Sol. A 81 (1984) 145.
[30] H.C. Liu, T.E. Mitchell, Acta Metall. 31 (1983) 863.
[31] H.C. Liu, C. Kinoshita, T.E. Mitchell, in: J.R. Holland, L.K. Mansur, D.I. Potter (Eds.), Phase Stability During Irradiation, Metallurgical Society of AIME, Warrendale, PA, 1981, p. 343.
[32] C. Dimitrov, B. Sitaud, X. Zhang, O. Dimitrov, O. Dedek, F. Dworschak, J. Phys.: Condens. Mater. 4 (1992) 10199.
[33] O. Dimitrov, C. Dimitrov, Intermetallics 2 (1994) 249.
[34] R. Sizmann, J. Nucl. Mater. 69&70 (1978) 386.
[35] C. Abromeit, R. Poerschke, J. Nucl. Mater. 82 (1979) 298.
[36] E.M. Schulson, J. Nucl. Mater. 83 (1979) 239.
[37] V. Naundorf, Int. J. Mod. Phys. B 6 (1992) 30.
[38] C. Abromeit, V. Naundorf, Intermetallics 4 (1996) 441.
[39] N. Njah, J. Nucl. Mater. 170 (1990) 232.
[40] E.P. Butler, J.F. Orchard, in: J.R. Holland, L.K. Mansur, D.I. Potter (Eds.), Phase Stability During Irradiation, Metallurgical Society of AIME, Warrendale, PA, 1981, p. 315.
[41] C. Abromeit, S. Müller, N. Wanderka, Scripta Metall. Mater. 32 (1995) 1519.
[42] C. Abromeit, S. Matsumura, PTM, Kyoto, 1999.
[43] R. Poduri, L.-Q. Chen, Acta Mater. 46 (1998) 1719.
[44] P.A. Stadelmann, Ultramicroscopy 21 (1987) 131.
[45] K.C. Russell, Prog. Mater. Sci. 18 (1984) 229.

[46] F. Soisson, P. Bellon, G. Martin, Phys. Rev. B 46 (1992) 11332.
[47] F. Soisson, P. Bellon, G. Martin, E. Salomons, J. Nucl. Mater. 205 (1994) 324.
[48] G. Martin, F. Soisson, P. Bellon, J. Nucl. Mater. 205 (1994) 301.
[49] H. Wollenberger, S. Matsumura, S. Müller, C. Abromeit, in: A. Gonis (Ed.), Stability of Materials, Plenum, New York, 1996, p. 687.
[50] S. Matsumura, Y. Tanaka, S. Müller, C. Abromeit, J. Nucl. Mater. 239 (1996) 42.
[51] S. Matsumura, M. Okudaira, C. Kinoshita, J. Nucl. Mater. 251 (1997) 145.
[52] F. Bourdeau, E. Camus, C. Abromeit, H. Wollenberger, Phys. Rev. B 50 (1994) 16205.
[53] E. Camus, C. Abromeit, Z. Metallkd. 85 (1994) 378.
[54] E. Camus, C. Abromeit, J. Appl. Phys. 75 (1994) 2373.
[55] E. Camus, F. Bourdeau, C. Abromeit, N. Wanderka, H. Wollenberger, Mater. Res. Soc. Symp. Proc. 373 (1995) 83.
[56] E. Camus, C. Abromeit, F. Bourdeau, N. Wanderka, H. Wollenberger, Phys. Rev. B 54 (1996) 3242.
[57] C. Abromeit, E. Camus, S. Matsumura, J. Nucl. Mater. 271&272 (1999) 246.
[58] A. Müller, V. Naundorf, M.-P. Macht, J. Appl. Phys. 64 (1988) 3445.
[59] G. Martin, Phys. Rev. B 30 (1984) 1424.
[60] G. Martin, P. Bellon, Solid State Phys. 50 (1997) 189.
[61] C. Abromeit, G. Martin, J. Nucl. Mater. 271&272 (1999) 251.